doi:10.1246/cl.2012.741
Published on the web June 30, 2012

Control of Periodicity in Mesoporous Silica Films with Aligned Mesochannels Prepared by a Sol–Gel Process

Atsushi Komoto, Wataru Kubo, and Hirokatsu Miyata*
Frontier Research Center, Canon Inc., 3-30-2 Shimomaruko, Ohta-ku, Tokyo 146-8501

(Received April 2, 2012; CL-120282; E-mail: miyata.hirokatsu@canon.co.jp)

Periodicity of mesoporous silica films with aligned cylindrical pores formed on a substrate with a rubbing-treated polyimide through a sol–gel process can be finely controlled using nonionic surfactants with different alkyl chains. The degree of alignment increases with the alkyl-chain length of the surfactant due to increase in anisotropic hydrophobic interaction between the oriented polyimide chains and the alkyl groups, which is responsible for the alignment.

Mesoporous silica (MPS) films are promising materials for application in optical and electronic molecular devices because they have highly ordered nanostructures and are synthesized through a simple self-assembly process.[1–5] Especially, MPS films with highly aligned cylindrical mesochannels are expected to be used for anisotropic accommodation of various guest species, e.g., metals,[6] dyes,[7] and polymers.[8,9] Several methods to control the alignment of the mesochannels have been reported.[10–17] Among them, the method in our previous report using a substrate with a rubbing-treated polyimide layer combined with evaporation-induced self-assembly (EISA) can control the mesochannel direction within the ϕ distribution of 3° at macroscopic scales.[11] The method, however, has not achieved to control the periodicity of the MPS films, which associates with the pore size. The optimum conditions for the preparation of aligned MPS films using different surfactants have been difficult to find because it is necessary to take the interactions between the oriented polyimide chains and the surfactant molecules into account in addition to the self-assembly of the surfactant. The control of the pore size of the aligned mesochannels enables the fine tuning of the properties of the guest species in the mesochannel through changes of the amount and the conformation. In view of this situation, we report the control of the periodicity and the pore size of the MPS films with aligned mesochannels by varying alkyl-chain length of nonionic surfactants.

The MPS films with the aligned mesochannels were prepared based on our previous method[11] after careful optimization for each surfactant. The polyimide with a 8-nm thickness on a Si wafer underwent rubbing treatment using a cotton-covered cylindrical roller. Nonionic surfactant (poly(oxyethylene)-10-alkyl ether, C_nEO_{10}, $n = 10$, 12, and 16) was dissolved in 2-propanol (IPA), and then ultrapure water (Milli-Q), 0.1 M HCl, and tetraethoxysilane (TEOS) were added to the solution. The final molar ratio of the chemicals was C_nEO_{10} 8.00×10^{-2}–0.120/TEOS 1.00/IPA 16.7/H_2O 5.00/HCl 4.00×10^{-3}. After stirring and aging the solution for 0.5–3.0 h, the Si wafer was dip-coated with the solution at withdrawal speed of 1.5 mm s^{-1} at 25 °C and 39–43% RH and subsequently dried at 25 °C and 40% RH over 16 h. The surfactants were removed by calcination at 400 °C for 10 h in air. Structural analysis of the synthesized films was performed by X-ray diffractometry (XRD). Conventional θ–2θ scanning XRD and in-plane XRD were performed with Philips X'Pert Pro and Rigaku ATX-G, respectively.

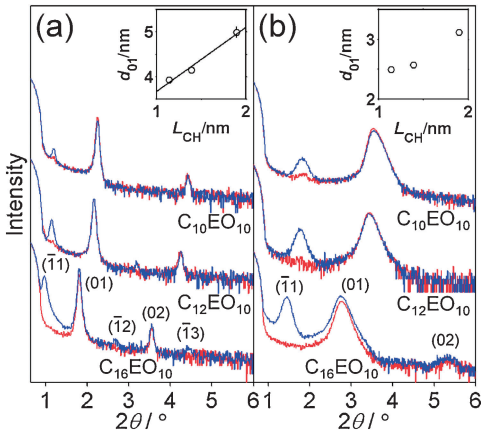

Figure 1. θ–2θ scanning XRD patterns of the (a) MSS and (b) MPS films. The directions of the incident X-rays are perpendicular (blue solid line) and parallel (red solid line) to the rubbing direction. Insets show d spacing of (01), d_{01}, plotted versus alkyl-chain length of the surfactants, L_{CH}. The solid line in the inset of (a) is a fitting line by a model of 2D hexagonal structure.

Figure 1 shows the θ–2θ scanning XRD patterns of the as-deposited mesostructured silica (MSS) films and the MPS films after removing the surfactants. Consistent with our previous report,[11] the XRD patterns indicate that the MSS and MPS films have 2D-hexagonal structure with the mesochannels parallel to the Si-wafer surface. These peaks shift and broaden after the calcination, resulting from the shrinkage of the film along the vertical direction and the consequent disordering of the periodic structure, respectively. The patterns recorded in the geometry with the projection of the incident X-rays perpendicular to the rubbing direction have extra peaks assigned to $(\bar{1}1)$, $(\bar{1}2)$, and $(\bar{1}3)$. These lattice points do not satisfy the Bragg conditions strictly but are observable due to the finite X-ray divergence angle comparable to the small diffraction angles of the films. The observed anisotropy suggests that the mesochannels in the films are macroscopically aligned as reported in our previous study.[18] The recorded XRD patterns show that the periodicity of the structure increases with the alkyl-chain length. Insets of Figure 1 summarize the relationship between the d spacing of (01), d_{01}, of the films and the alkyl-chain length of the surfactant, L_{CH}, which are calculated using MOE software (Chemical Computing Group Inc.). The d_{01} values of the MSS films can be fitted by a linear expression of L_{CH} obtained from a model of mesochannels packed and arranged in a regular hexagonal grid

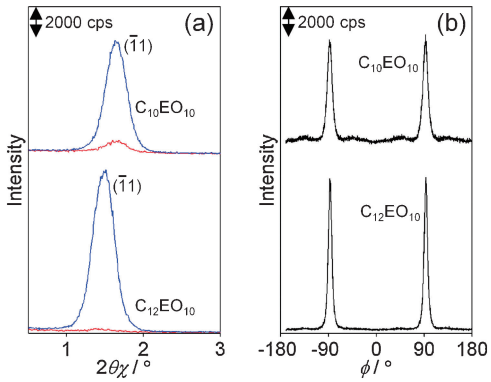

Figure 2. In-plane XRD study of the MPS films synthesized using $C_{10}EO_{10}$ and $C_{12}EO_{10}$. (a) ϕ–$2\theta\chi$ scanning XRD patterns: The projection of the incident X-rays is perpendicular (blue solid line) and parallel (red solid line) to the rubbing direction. (b) ϕ scanning rocking curves at $2\theta\chi$ peaks of the $(\bar{1}1)$ diffraction spots.

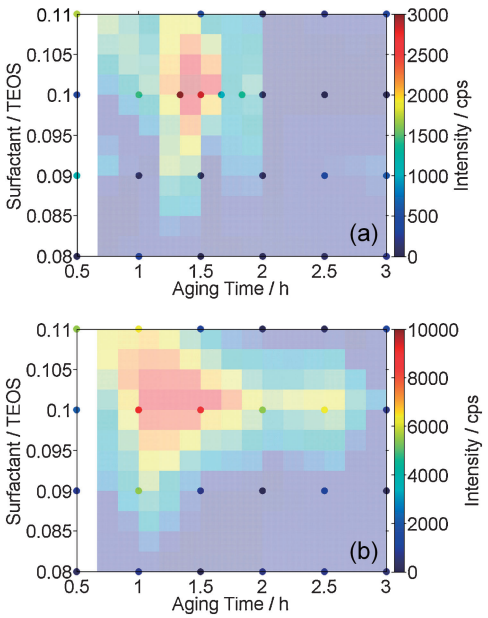

Figure 3. Visualization of the relationship between the structural anisotropy and the synthetic conditions for the MSS films using (a) $C_{10}EO_{10}$ and (b) $C_{12}EO_{10}$. The color shows the intensity of the diffraction spot assigned to $(\bar{1}1)$. The experimental data are shown as the filled circles and the intensity values between the data are estimated by linear interpolation.

(see Figure S2 in Supporting Information).[21] Radius of the mesochannel, r, distance between the adjacent mesochannels, a, and d_{01} obey the following equation due to their geometry in the regular hexagonal grid:

$$d_{01} = \frac{\sqrt{3}}{2}(2r + a) \quad (1)$$

Taking into account the structure of the used nonionic surfactants, the internal region of the mesochannels predominantly consists of alkyl chains. Therefore, r should be proportional to L_{CH}, that is, $r = \beta L_{CH}$, where β is a proportional constant, which indicates the folding degree of the alkyl chain. Finally, we can obtain the following equation:

$$d_{01} = \frac{\sqrt{3}}{2}(2\beta L_{CH} + a) \quad (2)$$

The experimentally obtained d_{01} values of the MSS films can be fitted by eq 2 which yields $r = 0.83L_{CH}$. This implies that the alkyl chains of the surfactants are slightly folded in the mesochannels.

Figure 2 summarizes the in-plane XRD study of the MPS films synthesized using $C_{10}EO_{10}$ and $C_{12}EO_{10}$. Figure 2a shows the ϕ–$2\theta\chi$ scanning profiles of the MPS films. The diffraction peaks assigned to $(\bar{1}1)$ can be observed clearly when the projection of the incident X-ray is perpendicular to the rubbing direction, as shown in our previous report.[11,18] In this study, we set the 2θ angle of the detector to that of the peak position of $(\bar{1}1)$ diffraction spot to maximize the intensity of this peak (see Supporting Information).[21] The positions and widths of the $(\bar{1}1)$ diffraction peaks are not changed through the calcination of the films (Supporting Information),[21] indicating that the horizontal periodicity is preserved.[11]

Figure 2b shows the ϕ scanning rocking curves at the $2\theta\chi$ peak positions of the $(\bar{1}1)$ diffraction spots. It is confirmed that the mesochannels in the MPS films are aligned perpendicularly to the rubbing direction ($\phi = 0°$). FWHM values of the peaks in the rocking curves are 11.3° for $C_{10}EO_{10}$ and 7.8° for $C_{12}EO_{10}$. These values are larger than the value for $C_{16}EO_{10}$ (2.8°), indicating that the degrees of the mesochannel alignment for $C_{10}EO_{10}$ and $C_{12}EO_{10}$ are lower than that for $C_{16}EO_{10}$. This is probably caused by the weaker hydrophobic interaction of $C_{10}EO_{10}$ and $C_{12}EO_{10}$ with the rubbing-treated polyimide surface due to their shorter alkyl chains.[8]

To find optimum synthetic conditions of the films with the aligned mesochannels, we performed a systematic analysis of the θ–2θ XRD profiles. We subtracted the profile recorded under the geometry in which the X-rays were parallel to the rubbing direction from that recorded under the perpendicular geometry, in order to extract the anisotropy of the diffraction peaks. The most remarkable difference is the diffraction peak assigned to $(\bar{1}1)$, which is observed only under the perpendicular geometry. The intensity of the $(\bar{1}1)$ peak, which is calculated by integrating the subtracted profile in the range of $0.95° \leq 2\theta \leq 1.35°$, can be used for evaluating the degree of the alignment of the mesochannels.

Figure 3 visualizes the dependence of the $(\bar{1}1)$ peak intensity on the synthetic conditions for the MSS films prepared using $C_{10}EO_{10}$ and $C_{12}EO_{10}$. The intensity data are plotted in a map with two parameters; the aging time of the solution and the surfactant/TEOS molar ratio. The intensity values between the experimental data are estimated by linear interpolation. These maps clearly show that the optimum surfactant/TEOS ratio and the aging time are 0.10 and 1.0–1.5 h, respectively. Compared to the optimum conditions for the aligned MSS film prepared with $C_{16}EO_{10}$, wherein the surfactant/TEOS ratio is 0.08 and the aging time is 2.0–3.0 h, these surfactants with shorter alkyl chains require higher surfactant concentration and shorter aging time. Again, it is also shown that the range of the optimum synthetic conditions for the aligned MSS film using $C_{10}EO_{10}$ is narrower than that using $C_{12}EO_{10}$. The difference in the

surfactant molar ratio would be attributed to the size difference of the surfactants. On the other hand, the shorter aging time in the conditions using $C_{10}EO_{10}$ and $C_{12}EO_{10}$ would be required from the optimization of the competing process between the rate of the micelle formation and the condensation rate of silica. To achieve the formation of a regular periodic mesostructure, the micelle-formation rate has to be larger than the silica-condensation rate.[19] The micelle-formation rates of $C_{10}EO_{10}$ and $C_{12}EO_{10}$ are thought to be lower than that of $C_{16}EO_{10}$ because their critical micelle concentrations (CMC) are much higher than that of $C_{16}EO_{10}$.[20] Therefore, to lower the rate of the silica condensation, the solution with a shorter aging time is favorable for preparing the MSS films with aligned mesochannels. However, too short aging times cause cracks in the MSS film. This is possibly because the condensation of siloxane oligomer is too small to bear the stress in the film caused by the rapid and drastic shrinkage during the coating process (see Supporting Information).[21]

In conclusion, the periodicity of the aligned MSS and MPS films can be controlled through the EISA process by varying the alkyl-chain length of the nonionic surfactant. Use of the surfactants with shorter alkyl chains results in broadening of the alignment distribution of the mesochannels because of its lower hydrophobic interactions with the rubbing-treated polyimide. The variation of the pore size of the aligned MPS films will enable the tuning of properties of the incorporated guest species.

References and Notes

1 M. Ogawa, *J. Am. Chem. Soc.* **1994**, *116*, 7941.
2 M. Endress, E. Zinner, A. Bischoff, *Nature* **1996**, *379*, 701.
3 Y. Lu, R. Ganguli, C. A. Drewien, M. T. Anderson, C. J. Brinker, W. Gong, Y. Guo, H. Soyez, B. Dunn, M. H. Huang, J. I. Zink, *Nature* **1997**, *389*, 364.
4 Y. Wan, D. Zhao, *Chem. Rev.* **2007**, *107*, 2821.
5 K. Ariga, A. Vinu, Y. Yamauchi, Q. Ji, J. P. Hill, *Bull. Chem. Soc. Jpn.* **2012**, *85*, 1.
6 T. Suzuki, H. Miyata, T. Noma, K. Kuroda, *J. Phys. Chem. C* **2008**, *112*, 1831.
7 A. Fukuoka, H. Miyata, K. Kuroda, *Chem. Commun.* **2003**, 284.
8 W. C. Molenkamp, M. Watanabe, H. Miyata, S. H. Tolbert, *J. Am. Chem. Soc.* **2004**, *126*, 4476.
9 I. B. Martini, I. M. Craig, W. C. Molenkamp, H. Miyata, S. H. Tolbert, B. J. Schwartz, *Nat. Nanotechnol.* **2007**, *2*, 647.
10 H. Miyata, T. Noma, M. Watanabe, K. Kuroda, *Chem. Mater.* **2002**, *14*, 766.
11 H. Miyata, Y. Kawashima, M. Itoh, M. Watanabe, *Chem. Mater.* **2005**, *17*, 5323.
12 T. Suzuki, Y. Kanno, Y. Morioka, K. Kuroda, *Chem. Commun.* **2008**, 3284.
13 B. Su, X. Lu, Q. Lu, X. Li, C. You, J. Jia, *Chem. Mater.* **2009**, *21*, 4970.
14 C.-W. Wu, T. Ohsuna, T. Edura, K. Kuroda, *Angew. Chem., Int. Ed.* **2007**, *46*, 5364.
15 N. A. Melosh, P. Davidson, P. Feng, D. J. Pine, B. F. Chmelka, *J. Am. Chem. Soc.* **2001**, *123*, 1240.
16 Y. Yamauchi, M. Sawada, T. Noma, H. Ito, S. Furumi, Y. Sakka, K. Kuroda, *J. Mater. Chem.* **2005**, *15*, 1137.
17 K. C.-W. Wu, X. Jiang, Y. Yamauchi, *J. Mater. Chem.* **2011**, *21*, 8934.
18 T. Noma, H. Miyata, K. Takada, A. Iida, *Adv. X-ray Anal.* **2002**, *45*, 359.
19 Q. Huo, D. I. Margolese, U. Ciesla, D. G. Demuth, P. Feng, T. E. Gier, P. Sieger, A. Firouzi, B. F. Chmelka, F. Schüth, G. D. Stucky, *Chem. Mater.* **1994**, *6*, 1176.
20 A. Berthod, S. Tomer, J. G. Dorsey, *Talanta* **2001**, *55*, 69.
21 Supporting Information is also available electronically on the CSJ-Journal Web site, http://www.csj.jp/journals/chem-lett/index.html.

